Analytical study on Class II Bragg resonance of surface wave interaction under the effect of current and surface tension

Deepali Goyal[a], **Tapan Kumar Hota**[b], **S.C. Martha**[a]
a. Department of Mathematics, Indian Institute of Technology Ropar, Punjab, India
b. Department of Mathematics, SRM University AP, Andhra Pradesh, India
*Corresponding authors: deepali.20maz0007@iitrpr.ac.in (DG), scmartha@iitrpr.ac.in (SCM)

HIGHLIGHTS

1. Class II Bragg resonance is investigated in a channel when the surface waves interact with bottom morphology of composite sinusoidal bars in the presence of current and surface tension.
2. A multi-scale expansion technique is used to obtain the expressions for reflection and transmission coefficients analytically with the advantage of uniformly valid solutions.
3. Current plays a very significant role in altering the Bragg resonance properties including the phase shift, amplitude and asymmetrical patterns in subharmonic peaks for reflection.
4. Depending upon current strength, number of ripples varies to attain almost 100% reflection.
5. The study is highly beneficial in the coastal areas where Bragg resonance occurs in the presence of ocean currents.

1 INTRODUCTION

Bragg resonance is the result of surface gravity waves interacting with a periodic bed morphology, such as sinusoidal bedform, to produce a resonant reflection of the waves. In oceanography, Bragg resonance is crucial for understanding how sandbars form erodible substrates and how manufactured bars protect coasts [1]. Literature involving composite sinusoidal beds have shown that the phenomenon goes beyond the basic Bragg resonances to encompass higher-order effects, such as harmonic and subharmonic Bragg reflections [2]. In addition to these composite sinusoidal beds, there is notable ocean current close to the coast due to wind, tides, and numerous other causes. This current can affect the morphologies of the coast and soil erosion while interacting with the ocean waves. Bragg resonance conditions are significantly influenced by currents, which also have an effect on wave interactions, resonant frequencies, and reflection. It is vital to comprehend the interactions and resonances that occur at different scales in a variety of research applications by using multi-scale analysis. As far as the authors are aware, the impact of surface tension and current on composite periodic beds (Class II Bragg resonance) that include all bottom interactions is still unclear. This work is crucial for the safety of coastal infrastructures and has the potential to further our knowledge of how currents affect coastal bathymetries of composite sinusoidal bars.

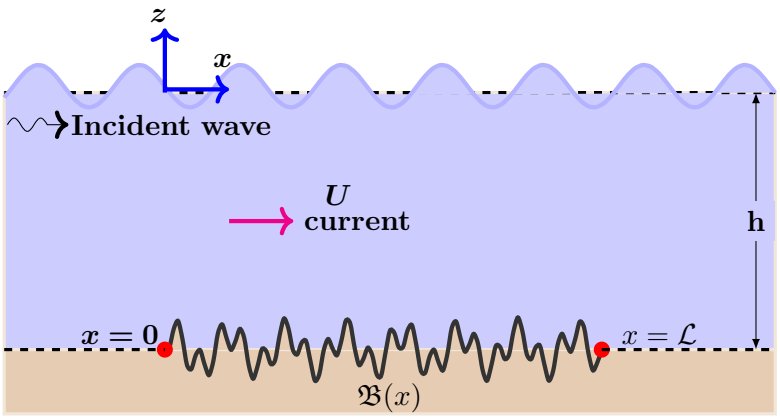

Figure 1: Schematic of propagation of surface wave in the presence of current U.

2 MATHEMATICAL FORMULATION

The schematic of the problem is given in Fig. 1. It is assumed that flow is irrotational and fluid is incompressible and inviscid. The wave with wavenumber k^* and angular frequency ω^* is incident normally on composite sinusoidal bars covering the region $[0, \mathcal{L}]$. Under the assumption of linearised water wave theory, the velocity potential $\Phi(x, z, t)$ satisfies the Laplace equation

$$\frac{\partial^2 \Phi}{\partial x^2} + \frac{\partial^2 \Phi}{\partial z^2} = 0, \quad -h + \epsilon \mathfrak{B}(x) < z < 0, \quad -\infty < x < \infty, \tag{1}$$

where h is mean water depth, $\epsilon\mathfrak{B}(x)$ is the variable depth characterised by composite sinusoidal bars above the mean depth $z = h$, and $\epsilon = O(D/h) \ll 1$ is a small parameter measures the ratio of bar amplitude to the depth. The composite sinusoidal bars can be expressed as

$$\mathfrak{B}(x) = \frac{-\mathrm{i}D_{b1}}{2} e^{\mathrm{i}K_{b1}x} + c.c \text{ of first term} + \frac{\mathrm{i}D_{b2}}{2} e^{-\mathrm{i}K_{b2}x} + c.c \text{ of second term.}, \quad 0 \le x \le \mathcal{L}, \tag{2}$$

where $\mathrm{i} = \sqrt{-1}$ and *c.c.* denotes the complex conjugate throughout the paper, the constants D_{b1} and D_{b2} are the ripple amplitudes and K_{b1} and K_{b2} (with $K_{b1} > K_{b2}$) are corresponding wave numbers of the composite sinusoidal bars. The combined free surface condition is given by

$$\left(\frac{\partial}{\partial t} + U\frac{\partial}{\partial x}\right)^2 \Phi + g\frac{\partial \Phi}{\partial z} = T\frac{\partial^3 \Phi}{\partial z \partial x^2} \quad \text{at } z = 0, \tag{3}$$

where g is gravity, U is current flowing in streamwise (x) direction and T is the surface tension. The bottom boundary condition is (see [1]):

$$\frac{\partial \Phi}{\partial z} = \epsilon\frac{\partial}{\partial x}\left(\mathfrak{B}\frac{\partial \Phi}{\partial x}\right) + \epsilon^2\frac{\partial}{\partial x}\left(\frac{\mathfrak{B}^2}{2}\frac{\partial^2 \Phi}{\partial x \partial z}\right) + \cdots, \quad z = -h. \tag{4}$$

3. MULTI SCALE ANALYSIS

For sub-harmonic resonance at $k^* = (K_{b2} - K_{b1})/2$, a multi-scale analysis is presented. The series of slow variables are introduced upto second-order as follows:

$$x_1 = \epsilon x, \; x_2 = \epsilon^2 x, \; t_1 = \epsilon t, \quad t_2 = \epsilon^2 t, \tag{5}$$

and the multi-scale expansion for solution can be expressed as

$$\Phi(x, z, t) = \epsilon\Phi_1(x, z, t, x_1, t_1, x_2, t_2) + \epsilon^2\Phi_2(x, z, t, x_1, t_1, x_2, t_2) + \epsilon^3\Phi_3(x, z, t, x_1, t_1, x_2, t_2) + \cdots \tag{6}$$

On using Eq. (6) expansion into boundary value problem (BVP) Eqs.(1)-(4), the series of BVPs upto third-order are obtained. The usual analysis will be excluded, and just the key findings will be summarized for third order. After solving the BVPs at first to third order, we obtain the solvability conditions at second and third order. Thus, the second-order and third-order solvability conditions [3] combine to give the coupled evolution equations for amplitudes of incident wave and reflected wave $\mathcal{A}^{\pm}(x, t)$, which can be written as

$$\frac{\partial \mathcal{A}^+}{\partial t} + c_g^*\frac{\partial \mathcal{A}^+}{\partial x} + \mathrm{i}\alpha^*\frac{\partial^2 \mathcal{A}^+}{\partial t^2} + \mathrm{i}\Omega_0^*\mathcal{A}^- + \mathrm{i}\Omega_1^*\mathcal{A}^+ = 0, \tag{7}$$

$$\frac{\partial \mathcal{A}^-}{\partial t} - c_g^*\frac{\partial \mathcal{A}^-}{\partial x} + \mathrm{i}\alpha^*\frac{\partial^2 \mathcal{A}^-}{\partial t^2} + \mathrm{i}\Omega_0^*\mathcal{A}^+ + \mathrm{i}\Omega_1^*\mathcal{A}^- = 0, \tag{8}$$

where

$$c_g^* = \left(\frac{(\omega^* - Uk^*)(1 + 2k^*h\,\mathrm{csch}\,2k^*h)}{2k^*} + U + \frac{k^{*2}T\tanh k^*h}{\omega^* - Uk^*}\right),$$

$$\alpha^* = \frac{[1+8k^{*2}h^2-\cosh 4k^*h+8k^*h(\sinh 2k^*h-2k^*h\cosh 2k^*h)](\omega^*-Uk^*)c_g^2}{4(\sinh 2k^*h+2k^*h)^2k^*\tanh k^*h(g+T_1k^{*2})c_g^{*2}}+\frac{c_gT_1k^{*2}}{k^*(g+T_1k^{*2})c_g^{*2}}+$$
$$\frac{(\omega^*-Uk^*)(-2k^{*2}T_1h-3k^*T_1\tanh k^*h+2k^{*2}hT_1\tanh^2 k^*h)}{2k^*c_g^{*2}(g+T_1k^{*2})\tanh k^*h}+\frac{k^{*2}T_1^2(\omega^*-Uk^*)}{2c_g^{*2}(g+T_1k^{*2})^2},$$
$$\Omega_0^* = -\frac{(\omega^*-Uk^*)k^*D_{b1}D_{b2}(k_{b1}+k_{b2})}{4\sinh 2k^*h}\times\frac{(\omega^*-Uk_1^+)^2\tanh k_1^+z+(g+T(k_1^+)^2)k_1^+}{(\omega^*-Uk_1^+)^2-(g+T(k_1^+)^2)k_1^+\tanh k_1^+h},$$
$$\Omega_1^* = \sigma_1^*D_{b1}^2+\sigma_2^*D_{b2}^2,\quad \sigma_j^* = -\frac{S_j^*(\omega^*-Uk^*)k^*\operatorname{csch}2k^*h}{4F^*(k_j^+)F^*(k_j^-)},$$
$$\begin{aligned}S_j^* =& -(\omega^*-Uk_j^+)^2(g+T(k_j^-)^2)k_j^-[k^*\cosh 2k^*h-k_{bj}\cosh 2k_{bj}h]\\ &-(\omega^*-Uk_j^-)^2(g+T(k_j^+)^2)k_j^+[k^*\cosh 2k^*h+k_{bj}\cosh 2k_{bj}h]\\ &+k_{bj}[(\omega^*-Uk_j^+)^2(\omega^*-Uk_j^-)^2-(g+T(k_j^+)^2)(g+T(k_j^-)^2)(k^{*2}-k_{bj}^2)]\sinh 2k_{bj}h\\ &+k^*[(\omega^*-Uk_j^+)^2(\omega^*-Uk_j^-)^2+(g+T(k_j^+)^2)(g+T(k_j^-)^2)(k^{*2}-k_{bj}^2)]\sinh 2k^*h,\end{aligned}$$
$$F^*(k_j^\pm) = (\omega^*-Uk_j^\pm)^2\cosh k_j^\pm h-(g+Tk_j^{\pm 2})k_j^\pm\sinh k_j^\pm h,\quad j=1,2.$$

We will further solve these Eqs. (7)-(8) to find the closed form solutions for complex wave amplitudes $\mathcal{A}^\pm(x,t)$. The evolution Eqs. (7)-(8) boil down to those of Fang et al. [1] when U and T are set to zero. The solutions for the amplitudes $\mathcal{A}^\pm$ of the coupled evolution Eqs.(7)-(8) can be assumed in the form of $\mathcal{A}^- = \mathcal{A}_0\mathcal{R}(x)e^{-\mathrm{i}\omega' t}$, $\mathcal{A}^+ = \mathcal{A}_0\mathcal{T}(x)e^{-\mathrm{i}\omega' t}$, in the region $0\le x\le\mathcal{L}$ where ω' is the detuned frequency. In the absence of modulated sinusoidal bars, the evolution Eqs.(7)-(8) are homogeneous, implying the boundary conditions $\mathcal{R}(\mathcal{L})=0$ and $\mathcal{T}(0)=1$. Hence, the reflection coefficient defined by $\mathcal{R}^* = |\mathcal{R}(0)|$ and transmission coefficient defined by $\mathcal{T}^* = |\mathcal{T}(\mathcal{L})|$ are respectively given by

$$\mathcal{R}^* = \sqrt{\frac{Q_1^{*2}}{Q_2^{*2}+P^{*2}\cot^2 P^*\mathcal{L}}},\qquad \mathcal{T}^* = \sqrt{\frac{P^{*2}\csc^2 P^*\mathcal{L}}{Q_2^{*2}+P^{*2}\cot^2 P^*\mathcal{L}}}. \tag{9}$$

where $P^* = \sqrt{Q_2^{*2}-Q_1^{*2}}$ with $Q_1^* = -\Omega_0^*/c_g^*$ and $Q_2^* = (\omega'-\alpha^*\omega'^2-\Omega_1^*)/c_g^*$.

4. NUMERICAL RESULTS

The influence of current U is illustrated in Fig. 2 by plotting the reflection coefficient $\mathcal{R}^*$ obtained from Eq. (9) for various values of U while maintaining constant values of $M=20, T=0$ dyne/cm, $D/h=0.2, h=2.5$ cm. It is observed from Fig. 2(a) that $\mathcal{R}^*$ decreased as the current speed U rises from 0 to 2.7 cm/s. The $\mathcal{R}^*$ decreases significantly to $\mathrm{O}(10^{-2})$ when the current speed is $U=2.7$ cm/s (see inset), revealing that the following current of $U=2.7$ cm/s tends to impede the reflected wave energy. At this value of current, it is additionally noticed (circle in the inset) that the left sub-harmonic peak, which is adjacent to the Bragg peak, hinders to an incredibly small value. This indicates that $\mathcal{R}^*$ in the immediate vicinity of the frequency at which Bragg peak occurs is significantly influenced by the currents flowing. The Bragg peak undergoes a rightward shift when the value of U increases, owing to the Doppler shift effect. From Fig. 2(b), it is seen that when current further increases from 2.75 cm/s to 2.81cm/s then the sub-harmonic peak amplitude is asymmetrical in nature i.e., left subharmonic peaks are increasing while right subharmonic peaks are decreasing. Also, the Bragg peak first shifts to left when current increases from 2.75 cm/s to 2.77 cm/s and then Bragg peak shifts to right when current increases from 2.77 to 2.81 cm/s. This means that this range of $U\in[2.75, 2.81]$ is highly sensitive as little increase in current shows very remarkable changes in the reflection coefficient. Further, in Fig. 2(c) when current increases from 3 cm/s to 4 cm/s, again reflection started to increase with Bragg peak shifting in right.

The effect of surface tension T and number of ripples M in the patch $[0, \mathcal{L}]$ are as follows (without figure): On increasing the surface tension T, reflection increases when $U \in [0, 2.81]$ and after that reflection decreases.
It is also observed in the study that with increase in number of ripples M, the solution remain bounded i.e., the solutions are uniformly valid since $\mathcal{R}^* \to 1$ as $M \to \infty$. However, for different current values, one requires different number of ripples to achieve maximum reflection. For instance if current $U = 1$ cm/s then $M = 80$ is sufficient to achieve 100 % reflection, if $U = 2.77$ then $M = 2000$ is required to achieve 100% reflection while for $U = 4$ cm/s one requires $M = 200$ ripples to achieve 100% reflection.

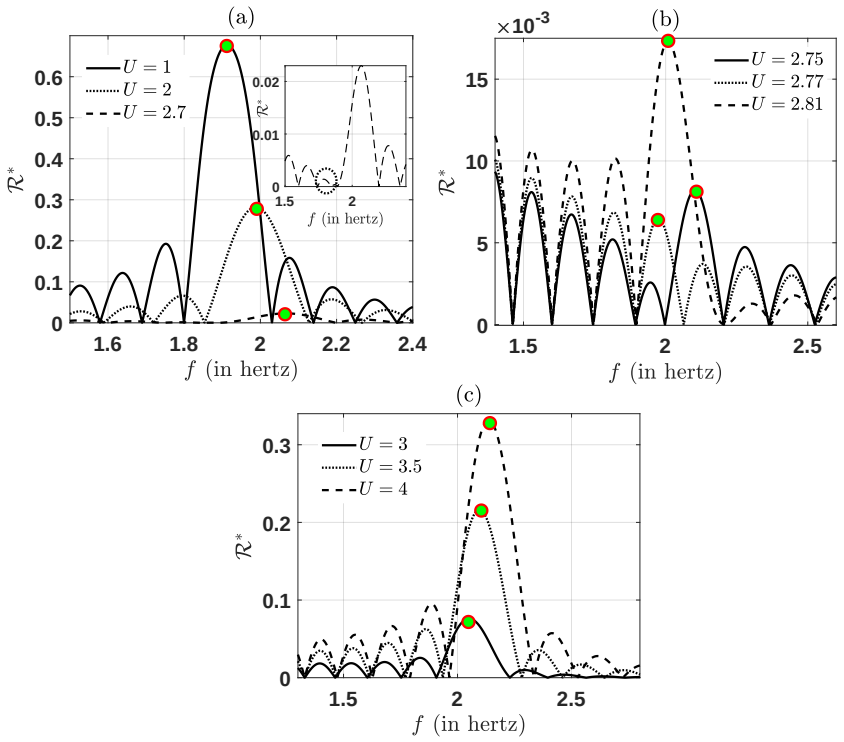

Figure 2: $\mathcal{R}^*$ versus frequency $f = \omega^*/2\pi$ (in hertz) for different U measured in cm/s. The filled circles denote resonant frequency where Class II Bragg resonance occurs.

5. CONCLUSIONS

An analytical solution for Class II Bragg resonance in the presence of ocean currents and surface tension is derived in this study through multi-scale analysis. The Bragg resonance found to be decreased when current U increases from 0 to 2.77 cm/s with phase shift towards right and for $U \in [2.77, 2.81]$ there occurs a sensitive region where highly asymmetrical patterns in the sub-harmonic peaks amplitude occur. Beyond this range, the Bragg peak started to increase as a consequence of negative relative group velocity. Also, the reflection coefficient converges to 1 when number of ripples M increases which shows that the solution is uniformly bounded. Moreover, depending upon the current range, number of ripples must be decided to achieve the 100% reflection.

Acknowledgement: DG (Award No.09/1005(0036)/2020-EMR-I) acknowledge CSIR, Govt. of India. SCM acknowledges the Science and Engineering Research Board, Department of Science and Technology, Govt. of India for the CRG grant (No. CRG/2023/008080).

REFERENCES

[1] Fang, H., Tang, L., and Lin, P. 2024. *Theoretical study on the downshift of class II Bragg resonance.* Physics of Fluids 36(1).

[2] Guazzelli, E., Rey, V., and Belzons, M. 1992. *Higher-order Bragg reflection of gravity surface waves by periodic beds. Journal of Fluid Mechanics 245*, 301–317.

[3] Mei, C. C. 1989. *The applied dynamics of ocean surface waves*, vol. 1. World Scientific Publishing, Singapore.